Study of the effect of F-Doping on lithium Electrochemical Behavior in $MnWO_4$ Anode Nanomaterials

Jianyu Wei[1], Jinxiu Ma[2], Wei Wang[3], Taohai Li[2, 5*], Na Wu[3]*, and Dabin Zhang[4]

Abstract

$MnWO_4$ nanorods with different contents of F-doping were synthesized by a facile approach. The morphological studies further confirmed formation of $MnWO_4$ nanorod structure with dimensional size and length of 50 nm and 100 nm, respectively. The differences of Li-storage performance that caused by F-doping contents in $MnWO_4$ nanomaterials were systematically investigated. The results show by tuning the F-doping contents in the $MnWO_4$ nanorods, both the reversible capacity and the cycling stability of nano-$MnWO_4$ electrode attain remarkable improvement. Furthermore when the content of F-doping is 0.05mol%, the reversible capacity for lithium storage in nano-$MnWO_4$ is at its maximum. What makes that all the more remarkable is that the 0.05mol% F-doped nano-$MnWO_4$ shows a long cycle life. Even cycled under a low current density (200mAh g^{-1}), the capacity retention still can keep more than 85% after 150 cycles, which are much superior to the report ones. These results provide insight into the effective method which can easily be applied to improve the electrochemical performances of the advanced electrode materials for Li ion batteries.

Keywords Batteries · Electrochemical energy storage ·Anode materials · F-doping · Nano-materials

1 Introduction

Facing the environmental degradation and energy crisis, it is a good way to concentrate on developing high energy density rechargeable batteries to solve the current problems.[1-8] Rechargeable lithium battery is among the rechargeable top energy systems in terms of both development and commercial application. To achieve the high energy density for rechargeable batteries, both the high specific capacity and low operating voltage of the electrode materials are very critical.[9-21] Thus as parts of these work, several recent studies have focused on developing high capacity anode materials (e.g. metallic lithium, silicon, and transition metal oxides, et al) in lithium-ion batteries.

During past decades transition metal tunstates, MWO_4, (M=Mn, Fe, Co, Ni, Cu, Zn, and Cd) have aroused much attention owing to their optic-based utilization[22]. Nowadays, MWO_4 have become promising anode material for lithium ion batteries because of its high lithium storage capacity and low voltage. Remarkably, many reports are available on synthesis of $MnWO_4$ nanomaterial with different morphologies. Recently, Mehdi Rahimi-Nasrabadi et al. produced $MnWO_4$ nanoparticles (NPs) through a co-precipitation procedure using various sugars as capping agents[23]. Ali Sobhani-Nasab et al. synthesized effectively a novel $MnWO_4$/$TmVO_4$[24] ternary nano-hybridse by using asimple sonochemical method and investigated for their photocatalytic performance. Most previous reports have mainly focused on synthesis of $MnWO_4$ nanomaterials with various morphologies and their characterization by physiochemical methods. Recently $MnWO_4$ and $MnWO_4$-based composites have been shown good potential in Li storage performance[33-35]. With the help of a conversion reaction ($MnWO_4 + 8Li^+ + 8e^- \leftrightarrow Mn + W + 4Li_2O$), $MnWO_4$ shows a relatively high specific capacity.[25-31]Among the different mixed metal oxide studied, tungstates of transition are the most promising materials which shows superior supercapacitive performance with good rate capability, large specific capacitance, and excellent cyclic performance[32]. Under the conversion reaction, it was perhaps inevitable that the large volume changes take places during the Li^+ insertion/extraction process. The most direct consequence due to large volume changes is that the electrode material becomes very unstable and the capacity fades rapidly. For high-performance batteries, cycling stability is as important as the specific capacity. So how to improve the cycle stability of the electrode materials is also a core work. Lots of work (e.g. carbon coating, foreign ions doping et al) has been done to improve the stability of the electrode materials.[38-40]Among them Fluorine (F)-doping has achieved good results benefiting from the intrinsic stability provided by F atom. [41-45] Fluorine (F)-doping stands out among them benefiting from the superior improvement effect on the electrochemical performance.[41-44]

[1] China Tobacco Guangxi Industrial Co., Ltd, Nanning, Guangxi 530001, PR China.

[2] Key Lab of Environment Friendly Chemistry and Application in Ministry of Education, College of Chemistry, Institution Xiangtan University, Xiangtan 411105, P. R. China, hnlth@xtu.edu.cn

[3] Key Laboratory of Inorganic Nanomaterials of Hebei Province, College of Chemistry and Material Science, Hebei Normal University, Shijiazhuang 050016, P. R. China,

[4] School of Mechanical Engineering, Guizhou University, Guiyang, Guizhou 550025, China

[5] Nano and Molecular Systems Research Unit, University of Oulu, P.O. Box 3000, FIN-90014, Finland

Though our groups have recently demonstrated the feasibility of promoting the Li storage property of $MnWO_4$ nano-electrodes by F-doping [46], more work still needs to be done systematically to investigate the effect of F-doped contents on Li storage performance. Herein, for the first time, a series of $MnWO_4$ nano-particles with different F-doped contents were synthesized by convenient hydrothermal reaction and evaluated the electrochemical property as Li-storage anode materials. Relations between the doping concentration and the insertion capacity and cycle stability were also studied for the $MnWO_4$ nano-electrodes. The result shows that the Li storage performance is increased significantly with the increasing contents of F^- doping and the amount of doping has an optimum value. When the contents of F-doping are larger than the optimum value, the Li storage performances drops sharply again. The nano-$MnWO_4$ with F-doping 0.05mol% delivers a highest Li reversible capacity of 708mAh g^{-1}, which is close to the theoretical capacity. In addition, when the F-doping contents were controlled in 0.05mol%, the $MnWO_4$ nano-electrode also owns excellent remarkable cycling stability with more than 85% capacity retention after cycled 150 cycles, which are far exceeding the previously reported ones.

2 Experimental Sections

2.1 Materials

Sodium tungstate dihydrate, manganese chloride, ammonium fluoride, anhydrous ethanol were obtained from China, and all reagents are analytical grade. Deionized water was used through all the experiments.

2.2 Synthesis of $MnWO_4$ nano-particles

1.00 mmol $MnCl_2$ was added into 15 mL water after 1.00 mmol Na_2WO_4 dissolved completely. Then above solution was titrated from pH 9.0 and transferred to an autoclave, which was sealed and heated at 180 °C for 12 h, and the mixture was allowed to cool naturally. The suspension was collected and washed three times with distilled water and ethanol. The dark brown precipitate was collected after dried at 80 °C for 24 h. Then the bare $MnWO_4$ is obtained.

2.3 Synthesis of F-doped $MnWO_4$ nano-particles

NH_4F (0.05 mol%, 0.10 mol%, 0.20 mol%, 0.25 mol%) is added into 15 mL water respectively with 1 g bare $MnWO_4$ dispersed forming solution A. Then the A solution is stirred for 30 min and transferred to an autoclave which was sealed and heated at 180 °C for 24 h. The suspension was collected and washed three times with distilled water and ethanol. The dark brown precipitate was collected after dried at 80 °C for 24 h. Then the F-doped $MnWO_4$ nano-particles are obtained.

2.4 Characterization

The Morphological determinations were performed on TEM (Tecnai F20). The powder X-ray diffraction (XRD) measurements were performed on a Regaku D/Max-2500. XPS measurement of samples was carried out with a ESCALAB 250Xi spectrometer. The Galvanostatic charge/discharge performance of samples was carried out between 0.05 to 3V under room temperature. Cyclic evoltammetry (CV) was measured in the potential range of 0.05-3 V (vs. Li^+/Li), whereas EIS was recorded in the frequency range of 10 MHz-100 kHz at an amplitude of 10 mV. The electrochemical performance of samples was tested by Swagelok-type cells with a Li metalic anode and LBC3401A4 (Capchem) electrolyte solution.

3 Result and Discussion

From the transmission electron microscopy (TEM) of the F-doped $MnWO_4$ samples, it can be seen clearly that the materials are gathered with a large number of short nanorods and have a uniform particle size distribution (Figure 1). And the morphology of the $MnWO_4$ with 0.25 mol% F-doping is also given in this paper (Figure 1e). By comparison, it was found that there is little difference between the sample with F-doping and the undoped one. This indicates that the morphology of $MnWO_4$ has no change after F-doping. Moreover, in Figure 1(g), the lattice spacing of 0.370 nm corresponds to the crystal plane of (110) in $MnWO_4$ (JCPDS: 74-1497). Whereas, in Figure 1(h), the lattice spacing of the $MnWO_4$ nanorods with 0.05mol% of F-doping is also bigger than that of the standard lattice spacing of (010) crystal plane of $MnWO_4$ (0.576nm), which indicates that the incorporation of F ion in $MnWO_4$ crystal lattice.

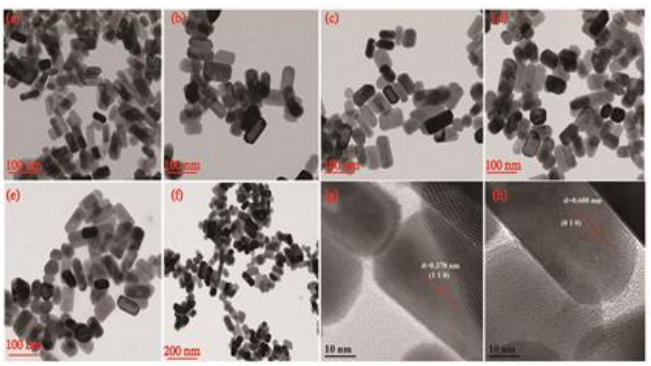

Figure1. TEM images of the nano-$MnWO_4$ with different contents of F-doping (a, f) 0mol%, (b) 0.05mol%, (c) 0.1mol%, (d) 0.2mol% (e) 0.25mol%, (g-h) High resolution TEM images of the nano-$MnWO_4$ with F-doping (g) 0mol%, (h)0.05mol%

The XPS and XRD characterization were carried out to

confirm the phase composition of the as-prepared materials. As shown in Fig. 2, the XRD peaks at angles of 18.4, 23.6 、29.9、30.3、36.1 and40.9° were indexed to (1 0 0), (0 1 1), (1 1 1), (- 1 1 1), (0 0 2) and (- 1 2 1) planes of $MnWO_4$, respectively (JCPDS card No.74-1497). The diffraction peaks of all the products are very complete and sharp, denoting the high crystallinities of the samples prepared in the solvothermal method. The diffraction peaks of the products are typical tungsten wolframite-type corresponding to the standard card of $MnWO_4$ (JCPDS card No. 74-1497). Moreover, as shown in Fig. 2b, the (- 1 1 1) peak of $MnWO_4$ obviously shift to lower angle, which indicates that the fluorine was doped into the lattice of $MnWO_4$. The XPS spectra (Figure 3a) show the characteristic peaks of F becomes stronger with the increase of the amount of doping. In order to preliminary analysis the F-doping effect, we have calculated the lattic parameters of the samples (Table 1). From the results the calculation, it was found that when the contents of F-doping increase, the lattice parameters also increase slightly.

This could be due to the partial reduction fromW^{6+} to W^{4+} to compensate for the charge of F^-. This has been demonstrated in the XPS characterization of W (Figure 3b). As $W6^+$ (0.60 Å) has smaller radius than W^{4+} (0.66 Å), the lattice parameters of the F-doped samples increases lightly with the increase of the amount of doping. Combining the XPS, XRD and TEM tests, which indicates that F ions were inserted into the interstices of the $MnWO_4$ lattice, resulting in expansion of the crystalline lattice.

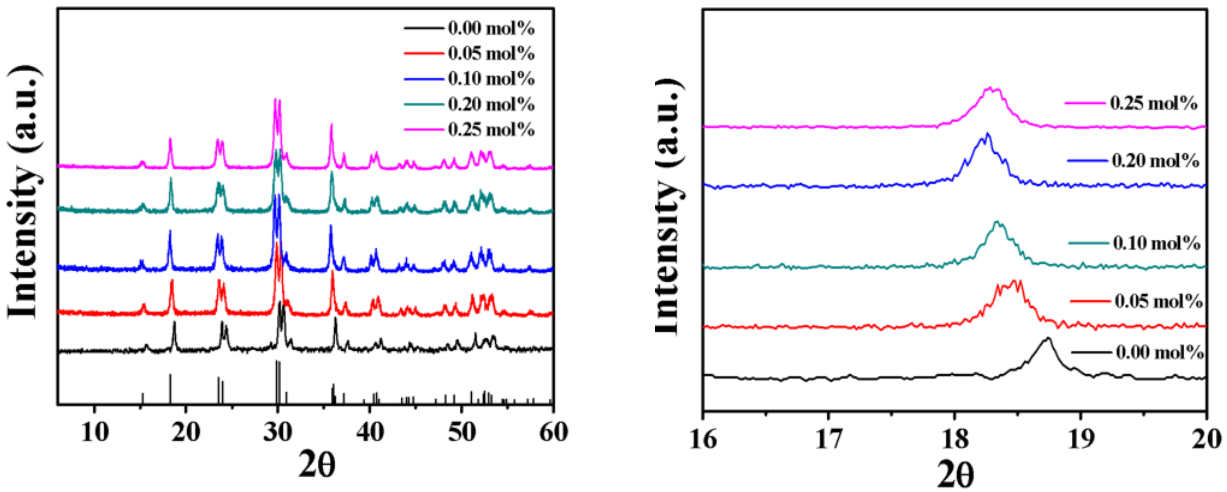

Figure2. (a) The XRD patterns (b) variations of (-111) peak position as a function of F doping concentrations

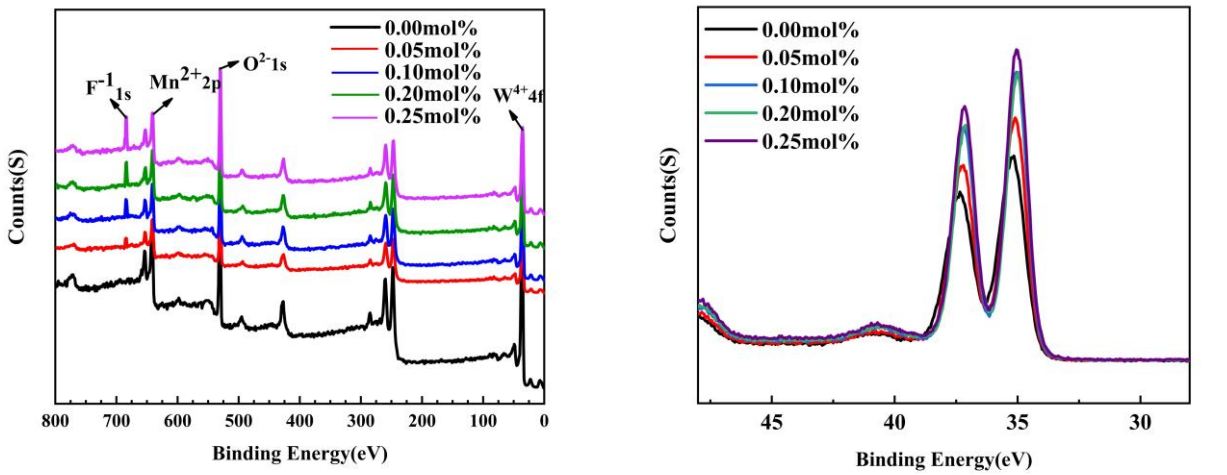

Figure3. (a) The XPS spectrum of samples, (b) The high-resolution XPS spectrum of the element W in the F-doped nano-$MnWO_4$

Table 1 Lattice and structural parameters for the $MnWO_4$ with different contents of F-doping

Samples	a(Å)	c(Å)	Unitcellvolume ($Å^3$)
F-doping(0.00mol%)	4.829	4.993	138.29
F-doping(0.05mol%)	4.830	4.996	138.72
F-doping(0.10mol%)	4.831	4.998	138.97
F-doping(0.20mol%)	4.833	4.999	138.99
F-doping(0.25mol%)	4.835	5.001	139.03

To evaluate the influence of F-doping on the electrochemical performance of the $MnWO_4$ electrodes with different F-doped contents, we carried out the electrochemical impedance spectroscopies (EIS) of the electrodes at different states (the pristine states Figure 4, discharge states Figure 5a and charge states Figure 5c) and also calculated the apparent Li diffusion coefficients (D_{Li}) to compare the Li -migration kinetics. Both the depressed semicircles in the medium-frequency region and the slanted lines in the low-frequency region appear on the Nyquist plots in Figure 5a and 5c. The depressed semicircles in the medium-frequency region are related to the charge-transfer process at the electrode/electrolyte interfaces.[50]And the so-called Warburg impedance (the slanted lines in the low-frequency region) reflects the Li diffusion in the crystal lattice.[51]With the increasing of the concentration of F-doping, the radius of the semicircles in Nyquist plots decreased indicating the impedances become smaller. However, when the contents of F doping are more than 0.05mol%, the impedances become larger. As shown in Figure 4 and 5, when the contents of F-doping is lower than 0.20mol%, the $MnWO_4$ electrodes have a significantly reduced charge transfer resistance (Rct) than the undoped one, implying the kinetics of the $MnWO_4$ electrode could be improved by F-doping.

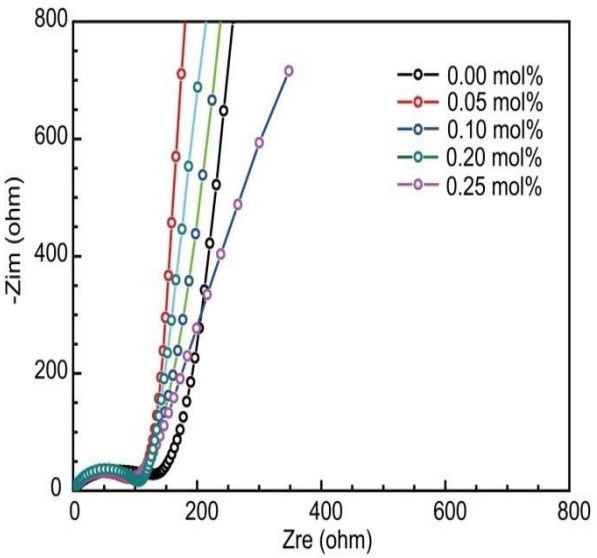

Figure4. The typical Nyquist plots of the $MnWO_4$ with different contents of F-doping at the pristine states

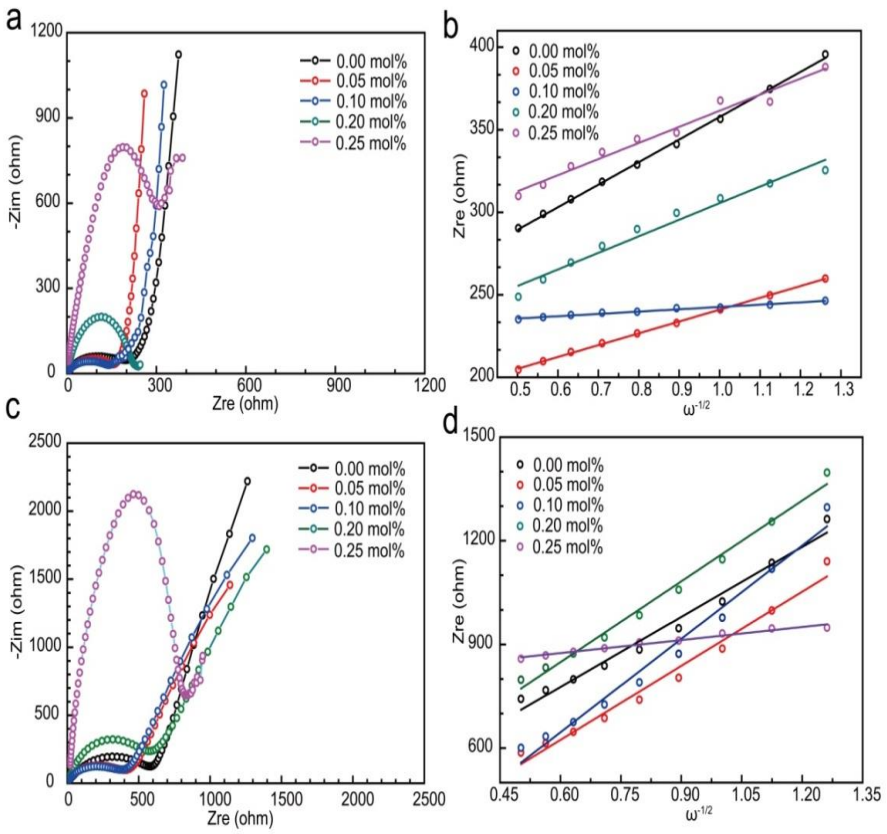

Figure5. (a. c) The Nyquist plots of the F-doped $MnWO_4$ cycled 5 times with discharge state (a) and charge state (c); (b, d) The variations and fittings between Zre and $\omega^{-1/2}$ (the reciprocal square root of the angular frequency) in low frequency region of the F-doped $MnWO_4$ cycled 5 times with discharge state (b) and charge state (d)

The apparent Li diffusion coefficients (D_{Li}) can be calculated according to Rct of the Nyquist plots from the incline lines in the low-frequency region by the following equation: $D_{Li}= R^2T^2/2A^2n^4F^4C^2\sigma^2$.

In the above equation, T means the absolute temperature, R is the gas constant, and A is on behalf of the electrode surface area, n and F represent the number of electrons per molecule during the reaction and the Faraday constant respectively.

C is the molar concentration of Li^+ ions, which can be calculated by the following formula.

C (mol cm^{-3}) = n_{Li} (mol)/V (cm^3) = [(I × t) C/1.6 × 10^{-19} C/6.02 × 10^{23} mol^{-1}]/V (cm^3) .here V is about 3 × 10^{-6} cm^3.

Finally σ is the Warburg factor, which is associated with Zre (Zre$\propto \sigma\omega^{-1/2}$).

After obtained the σ by linear fitting the relation plot between Zre and the $\omega^{-1/2}$, the D_{Li} could be obtained. The calculated D_{Li} values of the $MnWO_4$ with different contents of F-doping at discharged states are about 1.6× 10^{-19} cm ^{2} S^{-1} (0 mol%), 7.4 × 10^{-19}cm ^{2} S^{-1}(0.05 mol%), 6.9× 10^{-19}cm ^{2} S^{-1} (0.10 mol%), 1.8× 10^{-19} cm ^{2} S^{-1} (0.20 mol%), 1.3× 10^{-19}cm ^{2} S^{-1} (0.25 mol%), and at the charged states are 1.9× 10^{-20} cm ^{2} S^{-1} (0 mol%), 2.9× 10^{-20} cm ^{2} S^{-1} (0.05 mol%), 2.0× 10^{-20} cm ^{2} S^{-1} (0.10 mol%), 1.8× 10^{-20} cm ^{2} S^{-1} (0.20 mol%) and 1.4 × 10^{-20}cm ^{2} S^{-1}(0.25 mol%). We can see clearly that the $MnWO_4$ electrodes with proper F-doping contents have larger D values than the without one. These results further imply that F-doping with appropriate contents indeed could improve the kinetics of the $MnWO_4$ electrodes.

The comparison of the CV curves in the 2nd cycle of the $MnWO_4$ electrodes with different contents of F-doping are presented in Figure 6a. We can see clearly that the characteristic peaks which correspond to the Li^+ ion insert/extract from the electrodes are similar to the previous report ones. [33-35]And after F-doping, the above characteristic peaks maintain their features. However the intensity of the reversible redox peaks have increased significantly and the potential polarization becomes lower after F-doping. These results further validate that F-doping $MnWO_4$ will have better dynamics performances than the undoped one. These results further validate that F-doping $MnWO_4$ will have better dynamics performances than the undoped one.

The lithium storage properties of the $MnWO_4$ electrodes with different contents of F-doping were further examined by the galvanostatic charge-discharge tests (Figure 6 b-c and Figure 7). From the galvanostatic charge-discharge voltage profiles (Figure 6b), it was found that the capacity of the $MnWO_4$ electrodes increases firstly and then decreases with the increase of F-doping. When the content of F-doping is 0.05mol%, the discharge and charge

capacities are the highest ones. On account of the irreversible formation of the SEI layer on the electrode surface, the 1st discharge capacity (998mAh g^{-1}) is larger than the theoretical specific capacity (708mAh g^{-1}). After the 1st cycle, the discharge and charge capacity for the 2nd cycle is about 830mAh g^{-1} and 708mAh g^{-1}, respectively. However without F-doping, the 1st capacity of the electrode is only 560mAh g^{-1} (discharge) and 341mAh g^{-1}(charge) as shown in Figure 6b. These results indicate that its good electrochemical properties of the $MnWO_4$ electrodes with different contents of F-doping, which was obviously higher than the previously reported $MnWO_4$ nanostructures, for instance $MnWO_4$ nanoparticles (the discharge capacity can also keep at ≈500mAh g^{-1}) [52], $MnWO_4$/RGO composite (the discharge and charge capacity is about 680mAh g^{-1} and 540mAh g^{-1}) [53] . From the long cycle tests (Figure 6c), we can find that an activation process appear during the cycling. The activation time and cycling stability varies with the amount of F-doping. The electrode with 0.05 mol% F-doping owns the maximum activation time and the most stable cycle performance. Even under a low current density of 200mAh g^{-1} for 150 times, more than 85 % of the maximum stable capacity with high coulombic efficiency (~100 %) still can be obtained. The cycling stability, retention was also higher than the previously reports based on tungsten nanostructures, for instance flower like WO_3 (83.7% after 100 cycles at 1 A g^{-1}) [54], $MnWO_4$ nanorods (50% after 100 cycles at 2 mA cm^{-2}) [23] . These results indicated good electrochemical cycling stability of the $MnWO_4$ electrodes with different contents of F-doping. When measured under different current densities, the cell using the $MnWO_4$ electrode with F-doped (0.05 mol%) shows the largest reversible capacity and good recoverability, which is far exceeding of the samples with other F-contents as anode material in LIBs (Figure 7). All these results show that F-doping with appropriate amount could be an effective and simple way to improve the electrochemical properties of the nano-$MnWO_4$ electrode.

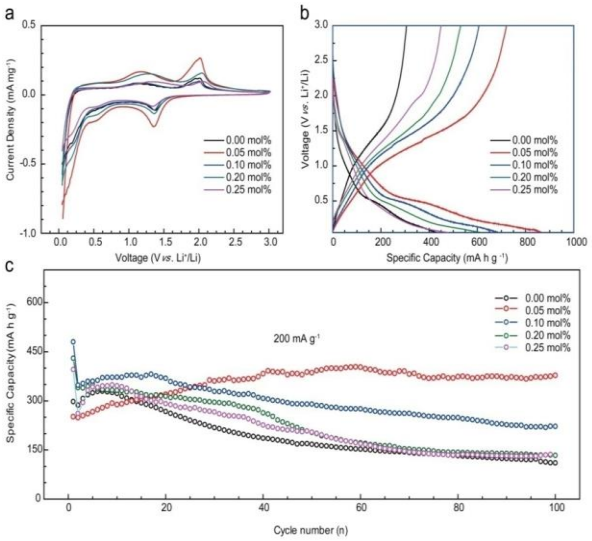

Figure6. (a) The CV curves in the second cycle at a scan rate of 0.1 mV S^{-1} in the voltage range of 0.01–3.0 V versus Li/Li^+ , (b) Galvanostatic discharge-charge voltage profiles measured under the current density of 15 mA g^{-1}, (c) Cycling performance of the nano-$MnWO_4$ electrodes with different contents of F-doping

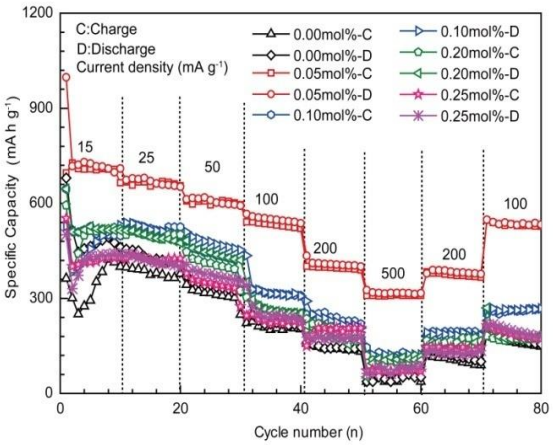

Figure7. The rate capability of the cell using F-doped nano-$MnWO_4$ electrodes with different contents of F-doping**.**

4 Conclusions

In conclusion, a series of nano-$MnWO_4$ with different contents of F-doping have been prepared by simple hydrothermal reaction. And the dependencies between lithium storage performance and the F-doped contents were systematically studied. The results show F-doping with appropriate content can act as simple and effective method to promote the electrochemical properties (e.g. the cycle stability, the reversible capacity).The $MnWO_4$ nanorods with 0.05 mol% F-doping deliver a highest capacity of 708mAh g^{-1} (the theoretical capacity) and a longest cycle life, as demonstrated that more than 85% capacity retention still can be received after 150 cycles. The outstanding electrochemical properties of the $MnWO_4$ nanorods with 0.05mol% F-doping may make it as a prospective

anode material for rechargeable Li batteries.

Conflicts of interest

There are no conflicts to declare.

Acknowledgment

The authors acknowledge with thanks the financial support of Hunan 2011 Collaborative Innovation Center of Chemical Engineering & Technology with Environmental Benignity and Effective Resource Utilization and the National Natural Science Foundation of China (51965009), the Natural Science Fundation of Hebei province (B2017205149), and the Hebei Provincial University Young Talent Program (BJ2017042) and Science and Technology Plan Project of Guizhou Province: [2019]5616.

References

1. J. B. Goodenough, Evolution of Strategies for Modern Rechargeable Batteries, Acc. Chem. Res, 46, 1053-1061 (2013)
2. M. Armand, S. Grugeon, H. Vezin, S. Laruelle, P. Ribiere, P. Poizot, J. M. Tarascon, Conjugated Dicarboxylate Anodes for Liion Batteries, Nat. Mater, 8, 120-125 (2019)
3. Y. Sun, N. Liu, Y. Cui, Promises and Challenges of Nanomaterials for Lithium-Based Rechargeable Batteries, Nat. Energy, 1, 16071 (2016)
4. D. H. Liu, H. Y. Lu, X. L. Wu, J. Wang, X. Yan, J. P. Zhang, H. Geng, Y. Zhang, Q. Yan, A New Strategy for Developing Superior Electrode Materials for A Compensate dvanced Batteries: Using a Positive Cycling Trend to the Negative One to Achieve Ultralong Cycling Stability, Nanoscale Horiz, 1, 496-501 (2016)
5. S. Xin, Y. G. Guo, L. J. Wan, Nanocarbon Networks for Advanced Rechargeable Lithium Batteries, Acc. Chem. Res, 45, 1759-1769 (2010)
6. Q. Wei, F. Xiong, S. Tan, L. Huang, E. H. Lan, B. Dunn, L. Mai, Porous One-Dimensional Nanomaterials: Design, Fabrication and Applications in Electrochemical Energy Storage, Adv. Mater, 1602300 (2017)
7. X. Z. Chen, H. Li, Thermodynamic analysis on energy densities of batteries, Energy Environ. Sci, 4, 2614-2624 (2011)
8. Y. Liang, R. Feng, S. Yang, H. Ma, J. Liang, J. Chen, Rechargeable Mg Batteries with Graphene-like MoS2 Cathode and Ultrasmall Mg Nanoparticle Anode, Adv. Mater, 23, 640-643 (2011)
9. Q. Xu, J. Y. Li, J. K. Sun, Y. X. Yin, L. J. Wan, Y. G. Guo, Watermelon-Inspired Si/C Microspheres with Hierarchical Buffer Structures for Densely Compacted Lithium-Ion Battery Anodes, Adv. Energy Mater, 6, 1601481 (2016)
10. T. Zhang, H. S. Zhou, A reversible long-life lithium-air battery in ambient air, Nat. Commun, 4, 1817 (2013)
11. Y. Zhang, P. Zhu, L. Huang, J. Xie, S. Zhang, G. Cao, X. Zhao, Few-Layered SnS2 on Few-Layered Reduced Graphene Oxide as Na-Ion Battery Anode with Ultralong Cycle Life and Superior Rate Capability, Adv. Funct. Mater, 25, 481-489 (2015)
12. T. Evans, D. M. Piper, S. C. Kim, S. S. Han, V. Bhat, K. H. Oh, S. H Lee, Ionic Liquid Enabled FeS_2 for High-Energy-Density Lithium-Ion Batteries, Adv. Mater, 26, 7386-7392 (2014)
13. H. H. Fan, H. H. Li, K. C. Huang, C. Y. Fan, X. Y. Zhang, X. L. Wu, J. P. Zhang, Metastable marcasite-FeS_2 as a new anode material for lithium ion batteries: CNFs-improved lithiation/delithiation reversibility and Li-Storage properties, ACS Appl. Mater. Interfaces, 9, 10708-10716 (2017)
14. T. T. Shan, S. Xin, Y. You, H. P. Cong, S. H. Yu, A. Manthiram, Combining Nitrogen-Doped Graphene Sheets and MoS_2: A Unique Film-Foam-Film Structure for Enhanced Lithium Storage, Angew. Chem. Int. Ed, 55, 2783-12788 (2016)
15. X. Zhu, X. Song, X. Ma, G. Ning, Enhanced Electrode Performance of Fe_2O_3 Nanoparticle-Decorated Nanomesh Graphene as Anodes for Lithium-Ion Batteries, ACS Appl. Mater. Interfaces, 6, 7189-7197 (2014)
16. Q. Wei, Y. Xu, Q. Li, S. Tan, W. Ren, Q. An, L. Mai, Novel Layered Li_3V_2 $(PO_4)_3$/rGO&C Sheets as High-Rate and Long-Life Lithium Ion Battery Cathodes, Chem. Commun, 52, 8730-8732 (2016)
17. H. B. Wu, G. Zhang, L. Yu, X. W. Lou, One-Dimensional Metal Oxide-Carbon Hybrid Nanostructures for Electrochemical Energy Storage, Nanoscale Horiz, 1, 27-40 (2016)
18. S. Guo, G. Lu, S. Qiu, J. Liu, X. Wang, C. He, H. Wei, X. Yan, Z. Guo, Carbon-Coated MnO Microparticulate Porous Nanocomposites Serving as Anode Materials with Enhanced Electrochemical Performances, Nano Energy, 9, 41-49 (2014)
19. S. Zhu, Q. Li, Q. Wei, R. Sun, X. Liu, Q. An, L. Mai, $NiSe_2$ Nanooctahedra as an Anode Material for High-Rate and Long-Life Sodium-Ion Battery, ACS Appl. Mater. Interfaces, 9, 311-316 (2017)
20. Q. Lian, G. Zhou, X. Zeng, C. Wu, Y. Wei, C. Cui, W. Wei, L. Chen, C. Li, Carbon Coated SnS/SnO_2 Heterostructures Wrapping on CNFs as an Improved-Performance Anode for Li-Ion Batteries: Lithiation-Induced Structural Optimization upon Cycling, ACS Appl. Mater. Interfaces, 8, 30256-30263 (2016)
21. Q. Wang, R. Zou, W. Xia, J. Ma, B. Qiu, A. Mahmood, R. Zhao, Y. Yang, D. Xia, Xu, Q. Facile Synthesis of Ultrasmall CoS_2 Nanoparticles within Thin N-Doped Porous Carbon Shell for High Performance Lithium-Ion Batteries, Small, 11, 2511-2517 (2015)
22. S. Pourmasoud, M. Eghbali-Arani, V. Ameri, et al. Synthesis of some transition MWO_4 (M: Mn, Fe, Co, Ni, Cu, Zn, Cd) nanostructures by hydrothermal method. J Mater Sci: Mater Electron, 30, 8105–8144 (2019).
23. Mehdi Rahimi-Nasrabadi et al., The effect of sugars on the morphology of $MnWO_4$ nanoparticles, and evaluating the product as photocatalysts, Journal of Materials Science, 28, 15239-15245 (2017)

24. Ali Sobhani-Nasab, Saeid Pourmasoud, Farhad Ahmadi, Marcin Wysokowski, Teofil Jesionowski, Hermann Ehrlich, Mehdi Rahimi-Nasrabadi, Synthesis and characterization of MnWO4/TmVO4 ternary nano-hybrids by an ultrasonic method for enhanced photocatalytic activity in the degradation of organic dyes, Materials Letters, 238, 159-162 (2019).
25. X. X. Wang, Y. Li, M. C. Liu, L. B. Kong, Fabrication and electrochemical investigation of MWO_4 (M = Co, Ni) nanoparticles as high-performance anode materials for lithium-ion batteries, Ionics, 1-10 (2010)
26. C. Gong, Y. J. Bai, J. Feng, R. Tang, Y. X. Qi, N. Lun, R. H. Fan, Enhanced electrochemical performance of FeWO4 by coating nitrogen-doped carbon, ACS Appl Mater Interfaces, 5, 4209-4215 (2013)
27. L. S. Zhang, Z. T. Wang, L. Z. Wang, Y. Xing, X. F. Li, Y. Zhang, Electrochemical performance of $ZnWO_4$/CNTs composite as anode materials for lithium-ion battery, J Mater Sci, 305, 179-185 (2014)
28. R. C. Pullar, S. Farrah, N. M. Alford, $MgWO_4$, $ZnWO_4$, $NiWO_4$ and $CoWO_4$ microwave dielectric ceramics, J Eur Ceram Soc, 27, 1059-1063 (2007)
29. V. K. V. P. Srirapu, A. Kumar, P. Srivastava, R. N. Singh, A. S. K. Sinha, Nanosized $CoWO_4$ and $NiWO_4$ as efficient oxygenevolving electrocatalysts, Electrochim Acta, 209, 75-84 (2016)
30. X. Y. Xu, J. P. Gao, G. B. Huang, H. X. Qiu, Z. Y. Wang, J. Z. Wu, Z. Pan, F. B. Xing, Fabrication of CoWO4@$NiWO_4$ nanocomposites with good supercapacitve performances. Electrochim, Acta. 174, 837-845 (2015)
31. G. J. He, J. M. Li, W. Y. Li, B. Li, N. Noor, K. Xu, J. Q. Hu, I. P. Parkin, One pot synthesis of nickel foam supported self-assembly of $NiWO_4$ and $CoWO_4$ nanostructures that act as high performance electrochemical capacitor electrodes, J Mater Chem A, 3, 14272-14278 (2015)
32. K. Adib, M. Rahimi-Nasrabadi, Z. Rezvani, et al. Facile chemical synthesis of cobalt tungstates nanoparticles as high performance supercapacitor. J Mater Sci: Mater Electron 27, 4541–4550 (2016).
33. H. W. Shim, A. H. Lim, J. C. Kim, G. H. Lee, D. W. Kim, Hydrothermal Realization of a Hierarchical, Flowerlike $MnWO_4$@MWCNTs Nanocomposite with Enhanced Reversible Li Storage as a New Anode Material Chem, Asian J, 8, 2851-2858 (2013)
34. E. Zhang, Z. Xing, J. Wang, Z. C. Ju, Y. T. Qian, Enhanced energy storage and rate performance induced by dense nanocavities inside $MnWO_4$ nanobars, RSC Adv, 2, 6748-6751 (2012)
35. M. Y. Ge, J. P. Rong, X. Fang, C. G. Zhou, Porous doped silicon nanowires for lithium ion battery anode with long cycle life, Nano Lett, 12, 2318-2323 (2012)
36. C. N. He, S. H. Wu, N. Q. Zhao, C. S. Shi, E. Z. Liu, J. J. Li, Carbon encapsulated Fe_3O_4 nanoparticles as a high-rate lithium ion battery anode material, ACS Nano, 5, 4459-4469 (2013)
37. C. Ban, Z. C. Wu, D. T. Gillaspie, L. Chen, Y. Yan. J. L. Blackburn, A. C. Dillon, Nanostructured Fe_3O_4/SWNT electrode: binder-free and high-rate li-ion anode, Adv Mater, 22, E145-E149 (2010)
38. Y. Ma, C. Fang, B. Ding, G. Ji, Y. J. Lee, Fe-Doped Mn_xO_y with Hierarchical Porosity as a High Performance Lithium-ion Battery Anode. Adv. Mater, 25, 4646-4652 (2013)
39. H. L. Poh, M. Pumera, p-Element-Doped Graphene: Heteroatoms for Electrochemical Enhancement, ChemElectroChem, 2, 190-199 (2015)
40. M. Y. Ge, J. P. Rong, X. Fang, C. G. Zhou, Porous doped silicon nanowires for lithium ion battery anode with long cycle life, Nano Lett, 12, 2318-2323 (2012)
41. J. Zheng, X. Wu, Y. Yang, Improved electrochemical performance of Li $[Li_{0.2}Mn_{0.54}Ni_{0.13}Co_{0.13}]O_2$ cathode material by fluorine incorporation, Electrochim. Acta, 105, 200-208 (2013)
42. L. Li, B. H. Song, Y. L. Chang, H. Xia, J. R. Yang, K. S. Lee, L. Lu, Retarded phase transition by fluorine doping in Li-rich layered $Li_{1.2}Mn_{0.54}Ni_{0.13}Co_{0.13}O_2$ cathode material, J. Power Sources, 283, 162-170 (2015)
43. H. Li, L. Z. Fan, Effects of fluorine substitution on the electrochemical performance of layered Li-excess nickel manganese oxides cathode materials for lithium-ion batteries, Electrochim. Acta, 113, 407-411 (2013)
44. H. G. Jung, C. S. Yoon, J. Prakash, Y. K. Sun, Mesoporous Anatase TiO_2 with High Surface Area and Controllable Pore Size by F-Ion Doping: Applications for High-Power Li-lon Battery Anode, J. Phys. Chem. C, 113, 21258-21263 (2009)
45. Y. Ma, B. Ding, G. Ji, J. Y. Lee, Carbon-Encapsulated F-Doped $Li_4Ti_5O_{12}$ as a High Rate Anode Material for Li^+ Batteries, ACS Nano, 7, 10870-10878 (2013)
46. W. Wang, N. Wu, J. M. Zhou, F. Li, Y. Wei, T. H. Li, X. L. Wu, $MnWO_4$ Nanoparticles as Advanced Anode for Lithium-ion Batteries: F-Doped Enhanced Lithiation/Delithiation Reversibility and Li-Storage Properties, Nanoscale, 10, 6832-6836 (2018)
47. Y. Deng, S. Tang, Q. Zhang, Z. Shi, L. Zhang, S. Zhan, G. Chen, Controllable synthesis of spinel nano-$ZnMn_2O_4$ via a single source precursor route and its high capacity retention as anode material for lithium ion batteries, J. Mater. Chem, 21, 11987-11995 (2011)
48. N. Sharma, G. V. S. Rao, B. V. R. Chowdari, Electrochemical properties of carbon-coated $CaWO_4$ versus Li, Electrochim. Acta, 50, 5305-5312 (2005)
49. R. Amin, P. Balaya, J. Maier, Anisotropy of Electronic and Ionic Transport in LiFePO4 Single Crystals, Electrochem. Solid-State Lett, 10, A13-A16 (2007)
50. X. L. Wu, Y. G. Guo, J. Su, J. W. Xiong, Y. L. Zhang, L. J. Wan, Carbon-Nanotube-Decorated Nano-$LiFePO_4$ @C Cathode Material with Superior High-Rate and Low-Temperature Performances for Lithium-Ion Batteries, Adv. Energy Mater, 3, 1155–1160 (2013)
51. J. Z. Guo, P. F. Wang, X. L. Wu, X. H. Zhang, Q. Yan, H. Chen, J. P. Zhang, Y. G. Guo, High-Energy/Power and Low-Temperature Cathode for Sodium-Ion Batteries: In Situ XRD Study and Superior Full-Cell Performance, Adv. Mater, 1701968 (2017)

52. F. Li, X. Xu, J. Huo, W. Wang, A simple synthesis of $MnWO_4$ nanoparticles as a novel energy storage material , Mater Chem Phys, 167, 22-27 (2015)
53. J. Tang, J. Shen, N. Li, M. Ye, Facile synthesis of layered $MnWO_4$/reduced graphene oxide for supercaacitor application, J Alloy Comp, 666, 15-22(2016)
54. J. Chu, D. Lu, X. Wang, S. Xiong, WO3 nanoflower coated with graphene nanosheet:synergetic energy storage composite electrode for supercapacitor application, J Alloy Comp, 702, 568-572 (2017)